Blm10 Protein Promotes Proteasomal Substrate Turnover by an Active Gating Mechanism

THE JOURNAL OF BIOLOGICAL CHEMISTRY VOL. 286, NO. 50, pp. 42830–42839, December 16, 2011

Blm10 Protein Promotes Proteasomal Substrate Turnover by an Active Gating Mechanism*[S]

Received for publication, September 1, 2011, and in revised form, October 21, 2011 Published, JBC Papers in Press, October 24, 2011, DOI 10.1074/jbc.M111.300178

Thomas Dange[‡1], David Smith[§2], Tahel Noy[‡], Philipp C. Rommel[‡3], Lukas Jurzitza[‡], Radames J. B. Cordero[‡], Anne Legendre[§4], Daniel Finley[§], Alfred L. Goldberg[§], and Marion Schmidt[‡5]

From the [‡]Department of Biochemistry, Albert Einstein College of Medicine, Bronx, New York 10461 and the [§]Department of Cell Biology, Harvard Medical School, Boston, Massachusetts 10115

Background: Association of the proteasome core with activators regulates proteasome activity.
Results: Blm10 association increases proteasome activity toward peptides and the unstructured proteasome substrate tau-441. This process is mediated by the C terminus of Blm10.
Conclusion: C-terminal docking-mediated proteasome activation by Blm10 facilitates the turnover of peptide and protein substrates.
Significance: Blm10 contributes to the regulation of proteasome activity.

For optimal proteolytic function, the central core of the proteasome (core particle (CP) or 20S) has to associate with activators. We investigated the impact of the yeast activator Blm10 on proteasomal peptide and protein degradation. We found enhanced degradation of peptide substrates in the presence of Blm10 and demonstrated that Blm10 has the capacity to accelerate proteasomal turnover of the unstructured protein tau-441 *in vitro*. Mechanistically, proteasome activation requires the opening of a closed gate, which allows passage of unfolded proteins into the catalytic chamber. Our data indicate that gate opening by Blm10 is achieved via engagement of its C-terminal segment with the CP. Crucial for this activity is a conserved C-terminal *YYX* motif, with the penultimate tyrosine playing a preeminent role. Thus, Blm10 utilizes a gate opening strategy analogous to the proteasomal ATPases Hb*YX*-dependent mechanism. Because gating incompetent Blm10 C-terminal point mutants confers a loss of function phenotype, we propose that the cellular function of Blm10 is based on CP association and activation to promote the degradation of proteasome substrates.

Regulated protein degradation by the ubiquitin-proteasome system is essential for the maintenance of eukaryotic protein homeostasis (1). The central component of this system is the 26S proteasome, a 2.5-MDa protease present in the cytoplasm and nuclei of eukaryotic cells (2). The proteasome is crucial for the removal of misfolded or damaged proteins, for providing building blocks for protein synthesis during nutrient limitation, and for the timed degradation of most short-lived proteins (3). The latter function is essential for the correct execution of many cellular processes including cell cycle control, transcription, translation, DNA repair, apoptosis, and antigen presentation (4). To execute its function as a universal protein degradation machinery, the proteolytic capacity of the proteasome is broad and for the most part indiscriminate. However, many control mechanisms regulate and limit proteasome function to prevent nonspecific protein degradation (5).

The 26S proteasome consists of two modules: a proteolytic core cylinder and a regulatory/activating module that binds to the core (2). The core (termed core particle (CP)[6] or 20S proteasome) is a barrel-shaped cylinder formed by four stacked rings (6). The two inner rings consist of seven homologous β-subunits each. Three of the β-subunits contain active sites with different substrate side chain preferences (7). The active sites face the interior of the core particle, thus creating a sequestered proteolytic chamber. The two outer rings are composed of seven homologous α-subunits, which provide docking sites for proteasome activators. To enter the internal degradation chamber, unfolded substrates must pass through the center of the α-ring. This pore is gated by the N termini of the α subunits (8), which must be displaced by proteasome activators (9).

The proteasome core interacts with three activator families: (*a*) complexes composed of or containing AAA+ ATPases (the eukaryotic regulatory particle (RP/19S/PA700) or the archaeal proteasome activating nucleotidase PAN); (*b*) the PA28/11S protein family, with PA28$\alpha\beta$ hetero-heptamers and the homo-heptameric PA28γ present in higher eukaryotes, as well as PA26 complexes found in *Trypanosoma brucei* (10, 11); and (*c*) the conserved Blm10/PA200 proteins found in all eukaryotes (9).

* This work was supported, in whole or in part, by National Institutes of Health Grants NIH-NIGMS-084228 (to M. S.), NIH-NIGMS-043601 (to D. F.), and NIH-NIGMS 5R01GM51923 (to A. L. G.). This work was also supported by the Multiple Myeloma Research Foundation.
[S] The on-line version of this article (available at http://www.jbc.org) contains supplemental Figs. S1–S3.
[1] Present address: Kavli Institute of NanoScience, Dept. of BioNanoScience, Technical University Delft, Lorentzweg, 2628 CJ Delft, The Netherlands.
[2] Present address: Dept. of Biochemistry, West Virginia University School of Medicine, 1 Medical Center Dr., Morgantown, WV 26506.
[3] Present address: Laboratory of Molecular Immunology, The Rockefeller University, HHMI, 1230 York Ave., New York, NY 10065.
[4] Present address: Dept. of Surgery and Interventional Science, University College London, 67 Riding House St., W1W 7EJ London, UK.
[5] To whom correspondence should be addressed: Dept. of Biochemistry, Albert Einstein College of Medicine, 1300 Morris Park Ave., Bronx, NY 10461. Tel.: 718-430-8868; Fax: 718-430-8565; E-mail: marion.schmidt@einstein.yu.edu.

[6] The abbreviations used are: CP, core particle; RP, regulatory particle.

Yeast Blm10 and its human ortholog PA200 (for proteasome activator with a molecular mass of 200 kDa) are monomeric proteasome activators that have been identified in hybrid complexes, where Blm10/PA200 occupies one end and the RP/19S the other end of the core cylinder (12–14). The same proteasome topology has been reported for PA28 family proteasome activators (15–18). Blm10/PA200 proteins are composed of HEAT repeats and display an elongated, curved tertiary structure (13, 19, 20). Similar to RP or PA28 binding, Blm10 or PA200 association with the CP enhances proteasomal peptidase activity (12, 13, 21), suggesting that proteasome activation is a conserved function for this class of proteins.

The 26 S proteasome and PA28–20S, Blm10, and PA200 proteasomes exhibit an open axial channel into the CP as demonstrated by cryo-electron microscopic studies (21, 22). These findings are supported by a recent x-ray structure of doubly capped reconstituted Blm10-CP complexes, which features a partially open, disordered CP gate (20). The structure also revealed that Blm10 binds to the CP via its C terminus, which occupies the same binding sites as PA26 and the proteasomal ATPases. From the position of the Blm10 C terminus within the binding pocket and its effect on the conformation of the outer surface of the α-subunit ring, it was proposed that gate opening by Blm10 might be achieved in a similar mechanism as suggested for the proteasomal ATPases (20).

Blm10 has been implicated in the final phase of CP maturation. It was identified in late stage CP assembly intermediates, yet deletion of *BLM10* does not result in a pronounced CP maturation defect (23). Loss of *BLM10*, however, in a mutant, which abrogates the association of the RP with CP (*sen3-1*) produced a marked proteasome maturation defect. These data suggest that the function of Blm10 during the final steps of proteasome maturation can be compensated by the RP and that activator binding to the CP in general is required for the final activation of the CP (23). After completion of proteasome biogenesis, Blm10 remains stably bound to the CP and affects the turnover of proteasome substrates (24).

We demonstrated recently that Blm10 is required for proteasome-mediated turnover of the transcriptional activator Sfp1 (24). Although Sfp1 protein levels increase upon loss of *BLM10 in vivo*, the turnover of Ubc6, a ubiquitin-dependent proteasome substrate, is not affected. These findings argue for a model in which Blm10 mediates the degradation of a specific subset of proteasome targets.

Sfp1 is a transcription factor required for the correct adaptation of ribosome biogenesis to the metabolic status of the cell, and the absence of Blm10 results in dysregulated ribosome biosynthesis. *BLM10* is strongly induced during oxidative growth or in the presence of rapamycin (24), which specifically inhibits TORC1 signaling, the major nutrient-sensitive signaling pathway. Deletion of *BLM10* furthermore causes partial mitochondrial dysfunction (20). These observations suggest that Blm10 proteasomes are involved in the regulation of metabolism.

Mechanistically, it is unclear whether these cellular functions are related to the physical interaction of Blm10 with the CP to activate proteasomal degradation of Blm10-specific substrates. Here we explore whether the described cellular functions of Blm10 could be tied to regulation of proteasome gating by studying the molecular details of proteasome activation by Blm10.

As described for PA26 and proteasomal ATPase binding, Blm10 association with the CP is mediated by its C terminus (20, 24). The C termini of Blm10 proteins contain a conserved motif, YY*X* or sometimes YF*X*, which is analogous to the C-terminal HbY*X* motif (where Hb indicates hydrophobic, and *X* is variable) in PAN and three (Rpt2, Rpt3, and Rpt5) of the six eukaryotic proteasomal ATPases (see Fig. 1 and Refs. 25 and 26). Biochemical and structural studies indicate that this motif is essential for ATPase-induced gate opening (25, 26, 29–31).

We show here that mutagenesis in that region of Blm10 produces a loss of function phenotype. Interestingly, a peptide derived from the last seven residues of Blm10 is sufficient to activate the CP peptidase activity, indicating that Blm10 opens the CP gate via a C-terminal docking mechanism, analogous to proteasomal ATPases. A peptide where the penultimate tyrosine was exchanged against an alanine, however, failed to activate the CP. Thus, this residue is crucial for Blm10-mediated proteasome activation.

An enzymatic characterization of proteasomal peptidase stimulation by Blm10 suggests that similar to its mammalian ortholog PA200 (12, 14), Blm10 activates the caspase-like and tryptic-like activity of the proteasome more strongly than the chymotrypsin-like activity. Lastly, we provide evidence that Blm10 proteasomes are competent to contribute to the turnover of cellular proteasome targets by demonstrating that Blm10 enhances proteasome-mediated degradation *in vitro* utilizing hypophosphorylated unstructured tau-441 as a substrate.

EXPERIMENTAL PROCEDURES

Strains—The strains used in this study are listed in Table 1. Genomically integrated C-terminal mutants were constructed by homologous recombination using standard techniques (27, 28) and were verified by sequencing. Primer sequences are available upon request.

Assay of Proteasomal Activity by C-terminal Peptides—Gate opening in yeast CP/20 S proteasome (0.2 μg/100-μl reaction) by C-terminal peptides was assayed in 50 mM Tris-HCl, 1 mM DTT, and 5% glycerol using the indicated fluorogenic substrates (100 μM Suc-LLVY-AMC, 50 μM Ac-nLPnLD-AMC, and 10 μM Suc-LRR-AMC) at 32 °C. The peptides derived from the C terminus of Blm10 (NH_2-VLWRSYYA-COOH), from the C terminus of PA26 (NH_2-GTDHMVS-COOH), and from the C terminus of PAN were synthesized by EZ Biolabs and were HPLC-purified to 98% purity. The peptides were dissolved in Me_2SO prior to addition to the reaction. The rate of substrate hydrolysis (AMC liberation) was monitored in a Spectramax M5 spectrophotometric plate reader by exciting at 380 nm and measuring emission at 460 nm.

Phenotypic Analysis—Strains were grown overnight in YPD and diluted in 96-well plates to a density of 6×10^6 cells/well followed by 5-fold serial dilutions. They were spotted onto YPD plates in the absence or presence of cycloheximide or on different carbon sources and incubated at the temperature indicated.

TABLE 1
Strains used in this study

BY4741	*MATa his3Δ1 leu2Δ0 met15Δ0 ura3Δ*	Ref. 52
yMS63	*MATa his3Δ1 leu2Δ0 met15Δ0 ura3Δ blm10Δ::NatMX*	Ref. 13
yMS94	*MATα his3Δ1 leu2Δ0 met15Δ0 ura3Δ blm10Δ::NatMX PRE1$_{TEV}$ProA (HIS3)*	Ref. 13
yMS122b	*MATa his3Δ1 leu2Δ0 met15Δ0 ura3Δ0 PRE1$_{tev}$ProA (HIS3) (KanMX)GAL1pHA3BLM10*	Ref. 13
yMS131	*MATα his3Δ1 leu2Δ0 met15Δ0 ura3Δ blm10Δ::NatMX*	This study
yMS152	*MATα his3Δ1 leu2Δ0 met15Δ0 ura3Δ0 blm10Δ::NatMX rpn4Δ::KanMX*	This study
yMS159	*MATα lys2-801 leu2-3,112 ura3-52 his3-A200 trpl-1 PRE1$_{TEV}$ProA(HIS3) ΔNα3 ΔNα7*	This study
yMS476	*MATa his3Δ1 leu2Δ0 met15Δ0 ura3Δ0 PRE1$_{TEV}$ProA(HIS3)*	This study
yMS598	*MATa his3Δ1 leu2Δ0 met15Δ0 ura3Δ blm10PA26C(KanMX)*	Ref. 24
yMS691	*MATα lys2-801 leu2-3,112 ura3-52 his3-A200 trpl-1 PRE1$_{TEV}$ProA (HIS3) ΔNα3 ΔNα7 blm10Δ::NatMX*	This study
yMS964	*MATα his3Δ1 leu2Δ0 lys2Δ0 ura3Δ0 (KanMX)GAL1pHA3BLM10*	This study
yMS966	*MATα his3Δ1 leu2Δ0 lys2Δ0 ura3Δ0 (KanMX)GAL1pHA3BLM10 rpn4Δ::HphMX*	This study
yMS968	*MATα his3Δ1 leu2Δ0 met15Δ0 ura3Δ0 (NatMX)GAL1pHA3blm10PA26C(KanMX) rpn4Δ::HphMX*	This study
yMS975	*MATα his3Δ1 leu2Δ0 met15Δ0 lys2Δ0 ura3Δ0 (NatMX)GAL1pHA3blm10PA26C(KanMX)*	This study
yMS976	*MATα his3Δ1 leu2Δ0 met15Δ0 ura3Δ*	This study
yMS977	*MATα his3Δ1 leu2Δ0 ura3Δ0 rpn4Δ::HphMX*	This study
yMS980	*MATa his3Δ1 leu2Δ0 met15Δ0 ura3Δ blm10S2140H(KanMX)*	This study
yMS981	*MATa his3Δ1 leu2Δ0 met15Δ0 ura3Δ blm10R2139D(KanMX)*	This study
yMS989	*MATa his3Δ1 leu2Δ0 met15Δ0 ura3Δ0 (NatMX)GAL1pHA3blm10PA26C(KanMX) PRE1$_{TEV}$ProA(HIS3)*	This study
yMS992	*MATa his3Δ1 leu2Δ0 met15Δ0 ura3Δ blm10Y2142V(KanMX)*	This study
yMS993	*MATa his3Δ1 leu2Δ0 met15Δ0 ura3Δ blm10Y2141M(KanMX)*	This study
yMS994	*MATa his3Δ1 leu2Δ0 met15Δ0 ura3Δ blm10A2143S(KanMX)*	This study

Analysis of Proteasome Complex Composition in Unfractionated Lysates—Proteasomal complexes in lysates were detected as described previously (13), with the exception that the lysis was performed by cryogenic disruption using a Retsch MM301 grinder mill. Equal total protein (200 μg) was loaded in each well.

Blm10 Proteasome Complex Purification—For the purification of WT and mutant Blm10-CP complexes, cells from yMS122 or yMS476 were collected and lysed by cryogenic disruption with a Retsch MM301 grinder mill. Purification was performed as described previously (13). Briefly, the cleared lysate was batch-incubated with IgG affinity gel (Cappel), and the beads were collected and washed. Proteasome complexes were eluted after cleavage with tobacco etch viral protease (Invitrogen). Subsequently, the purified complexes were first resolved on 3.5% acrylamide native gels (13), followed by an in-gel activity assay with the fluorogenic proteasome substrate Suc-LLVY-AMC as described previously (13) and SDS-PAGE followed by Sypro Ruby staining to assess complex composition and purity of the sample.

Proteasome Activity Assay—Three different fluorogenic peptide substrates were used to analyze proteasomal activity: Suc-LLVY-AMC (12.5–200 μM), Ac-RLR-AMC (12.5–350 μM), and Ac-nLPnLD-AMC (12.5–350 μM). All of the substrates were purchased from BACHEM and prepared as 40× stock solutions in Me_2SO. Activity was assessed in 96-well assay plates (Costar 3631) by monitoring the kinetics of fluorescence increase of generated free AMC in a plate reader (Spectramax M5; excitation, 380 nm; emission, 460 nm). The assay buffer contained 50 mM Tris, pH 7.5, 5 mM $MgCl_2$, 0.5 mM EDTA. Purified CP and Blm10-CP were used at a final concentration of 1 nM. The assay mixture was preincubated for 15 min at 30 °C. Fluorescence increase was recorded at an interval of 30 s for 30 min with 5 s of mixing prior to each cycle. The data were analyzed with GraphPad Prism 5 to calculate the corresponding values of K_{half}, V_{max}, and R^2. The equation was adapted from R. A. Copeland as provided on the GraphPad webpage.

In Situ Analysis of Blm10-CP Complex Activity—5 μg of purified CP and Blm10-CP were separated on a 3.5% polyacrylamide native gel. For the in-gel activity assay, the gel was incubated in 50 mM Tris, pH 7.4, 5 mM $MgCl_2$, 1 mM ATP, 100 μM Suc-LLVY-AMC (Bachem) for 10 min at 30 °C. Activity was assessed by visualizing AMC fluorescence after proteasomal cleavage of LLVY-AMC on an ultraviolet screen. Subsequently, the total protein concentration was assessed using SYPRO Ruby Protein stain (Invitrogen) following the manufacturer's instructions. The same samples were analyzed by immunoblotting using anti-Blm10 (this study) and anti-proteasome 20 S core subunits (BioMol) antibodies. Images were taken on an EL Logic 100 imaging system (Kodak). For signal quantification, analysis was performed using the software ImageJ 1.41o. CP activity was corrected for the protein abundance in each individual band.

In Vitro Degradation of Tau—Reaction mixtures contained 0.5 mM EDTA, 5 mM $MgCl_2$, 50 mM Tris-HCl, pH 7.4, and 600 nM recombinant tau-441 (recombinant human tau variant 2N4R; Enzo Life Sciences) in a final volume of 15 μl. The reactions were supplemented with 1 nM of CP or Blm10-CP in the absence or presence of 40 μM MG132 (CalBiochem) as indicated. The reactions were incubated at room temperature, and samples were taken at the indicated time points and boiled for 5 min with ELPHO sample buffer to terminate the reactions, followed by immunoblot analysis with anti-tau antibody (BIOSOURCE). The signals were recorded using an ImageQuant LAS 4000 and analyzed by densitometry with the Image Quant software.

RESULTS

The Role of the C-terminal Residues of Blm10 in CP Binding and Activation—Sequence identity among Blm10 orthologs is as low as 17% (human *versus* yeast) (12). The physicochemical features of the C-terminal residues on the other hand are highly conserved (Fig. 1*A*). The last residue is always hydrophobic (Ala, Val, and Ile), and the penultimate is always aromatic (Phe or Tyr), whereas the preceding residue is always a Tyr. This motif thus resembles the Hb*YX* motif in proteasomal ATPases and in the archaeal PAN (Fig. 1*A*) (29), which has been demonstrated to trigger gate opening. We have shown previously that

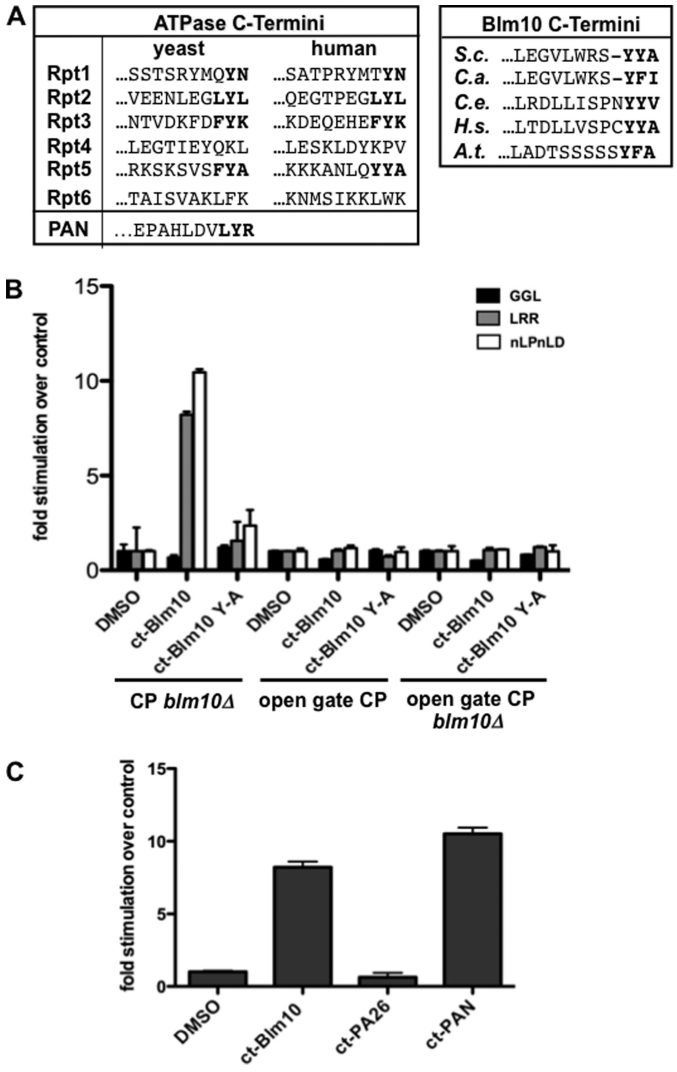

FIGURE 1. **The C terminus of Blm10 stimulates the CP peptidase activity and thus mediates gate opening.** *A*, *left panel*, sequence alignments of the C-terminal segments of *S. cerevisiae* (yeast), human, and archaeal (*M. jannaschii*, PAN) proteasomal ATPases. HbYX motifs are indicated in *bold letters*. *Right panel*, sequence alignments of the C-terminal segments of Blm10 orthologs. *S.c.*, *Saccharomyces cerevisiae*; *C.a.*, *Candida albicans*; *C.e.*, *Caenorhabditis elegans*; *H.s.*, *Homo sapiens*; *A.t.*, *Arapidopsis thaliana*. *B*, heptapeptides derived from the wild-type Blm10 C terminus (ct-Blm10), as well as a peptide where the penultimate tyrosine has been replaced by alanine (ct-Blm10 Y-A) were tested for their ability to stimulate CP peptidase activity against three fluorogenic peptides assaying the chymotryptic (Suc-GGL-AMC), the tryptic (Suc-LRR-AMC), and the caspase-like activity (Ac-nLPnLD-AMC) of the proteasome. The assays were performed with 0.2 μg of purified wild-type CP and an open gate mutant, where the N termini of α3 and α7 were deleted. The open gate mutant was purified from either WT cells or cells deleted for *BLM10*. The data are normalized for the activity of wild-type CP with the respective substrate. *C*, to compare ct-Blm10-mediated stimulation with ct-PAN and ct-PA26, the same assay as in *A* was performed with Suc-LRR-AMC, the proteasome substrate that showed the highest stimulation for the C-terminal peptide of Blm10. *DMSO*, dimethyl sulfoxide.

the last three residues of Blm10 are required for CP binding and its function *in vivo* (24). Because CP gate opening can be induced by peptides derived from the eukaryotic ATPases Rpt2 and Rpt5 or from the archeal ATPase PAN (29–31), we speculated that the C-terminal peptide of Blm10 (ct-Blm10) might be sufficient to induce gate opening and thus to stimulate CP peptidase activity.

We tested this hypothesis with a WT Blm10 C-terminal peptide encompassing the last seven residues (ct-Blm10) and a control peptide where the penultimate tyrosine was substituted with alanine (ct-Blm10Y-A). This conserved residue is critical for RP- and PAN-induced gate opening (29). We found that the C-terminal peptide markedly stimulated the hydrolysis of fluorogenic peptide substrates of the proteasome's trypsin-like (LRR-AMC) and the caspase-like (nLpnLD-AMC) activity (Fig. 1*B*). Because these substrates are cleaved by different sites and because their hydrolysis is limited by their entry rate, these findings suggest that Blm10 activates gate opening. Accordingly, the activity of a mutant CP with a constitutively open gate caused by N-terminal truncations at two of the α-subunits involved in the gating process (8) was not stimulated by ct-Blm10 (Fig. 1*B*). These data strongly suggest that the increased peptide hydrolysis by the CP, observed in the presence of ct-Blm10, is caused by gate opening and not direct stimulation of CP active sites. Furthermore, an exchange of the penultimate tyrosine in the peptide (ct-Blm10 Y-A) abrogated CP activation, confirming a crucial function either in CP binding or gate opening for this residue. The overall capacity of ct-Blm10 to stimulate yeast CP activity was comparable with that of the C-terminal peptide of PAN (ct-PAN), whereas the gating-incompetent C terminus of PA26 (ct-PA26) was ineffective in stimulating yeast CP (Fig. 1*C*), in accordance with results obtained for mammalian CP (29). In contrast to the trypsin-like or caspase-like activity, we did not observe stimulation of the chymotrypsin-like activity with ct-Blm10, which is consistent with data reported for the C termini of the proteasomal ATPases (29).

To further characterize the role of the C-terminal residues, we constructed genomically integrated point mutations where the last five residues were substituted with the residues corresponding to the same positions in PA26. Because the PA26 C terminus binds to the same pockets as Blm10, this strategy is expected to minimize structural disturbances during CP docking. We have shown previously that Blm10 is required for correct repression of ribosome biogenesis and that *BLM10* deleted cells exhibit cycloheximide resistance at low concentrations of this translation inhibitor (24). We therefore tested whether the C-terminal mutants produce a loss of function phenotype and found that an exchange of the penultimate tyrosine (Y2142V) indeed mimicked *BLM10* deletion, showing increased viability with cycloheximide present (Fig. 2*A*). A similar increase in viability was observed for S2140H, whereas a partial loss of function phenotype is observed for R2139D (Fig. 2*A*). Mutation of the last residue (A2143S) or Y2141M had no effect on viability in the presence of cycloheximide. To explore whether the phenotypes were caused by disrupted Blm10-CP interaction, we studied the relative distribution of proteasomal complexes in unfractionated lysates after native gel separation followed by an in-gel activity assay. Y2142V and S2140H mutations abrogated binding, which was preserved in R2139D (Fig. 2*B*). We speculate that the partial loss of function phenotype of the latter mutant is caused by an impaired gating mechanism. These findings are in agreement with previously published data, which revealed that the deletion of the last residue of Blm10 or the substitution of the last seven residues with the gating incompetent PA26 C-terminal peptides allowed CP binding yet produced a loss of function phenotype (24).

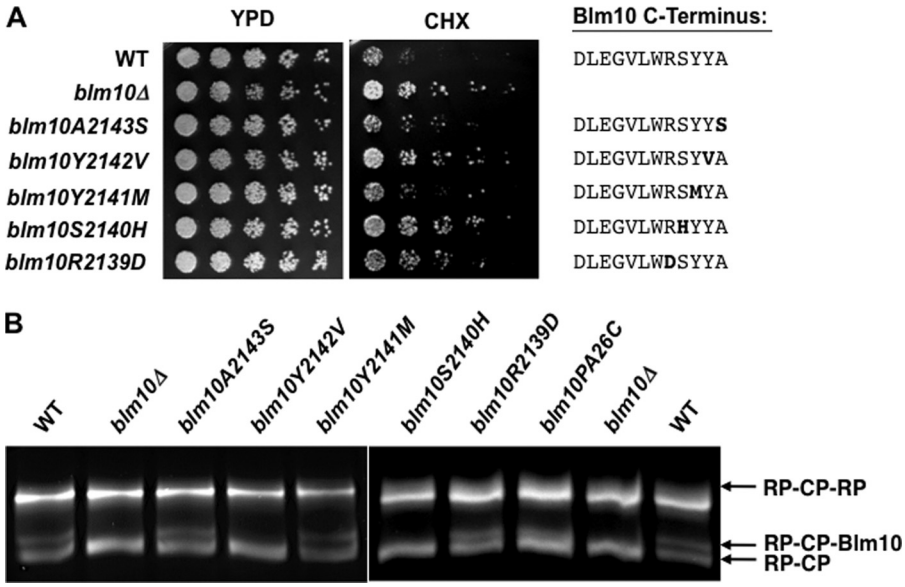

FIGURE 2. **The penultimate tyrosine within the Blm10 YYX motif is required for proteasome binding.** *A*, WT, *BLM10* deleted cells (*blm10*Δ), and genomically integrated point mutants within the last five residues of Blm10 as indicated by *bold letters* to the right were spotted on YPD plates in the absence (*left panel*) or in the presence of 0.3 μg cycloheximide (*right panel*) and were grown for 3–5 days at 30 °C. The C-terminal sequences are indicated to the *right*. *B*, the same strains as in *A* were tested for proteasome association in unfractionated lysates. The cell lysates were separated by native gel electrophoresis. Active proteasomes are visualized by an in-gel activity assay using Suc-LLVY-AMC.

The Impact of Blm10 on Enzymatic Activities of the Proteasome—The C-terminal Blm10 peptide impacted the different proteasomal peptidase activities of the CP differentially. Although the chymotrypsin-like activity remained largely unaffected, the trypsin-like and the caspase-like activities were elevated (Fig. 3). Differential stimulation has also been observed for purified PA200–20S complexes (12). To test whether the effects obtained with ct-Blm10 are also observed with the endogenous Blm10-CP complex, they were purified and subjected to a detailed enzymatic analysis. We obtained essentially the same results as for the ct-Blm10 stimulated CP peptidase activities: stimulation of trypsin-like and caspase-like activities, but unaffected chymotrypsin-like activity (Fig. 3). Prior studies have in fact shown that chymotrypsin-like fluorogenic peptide substrates can induce gate opening (32), and because of their very rapid cleavage by the chymotrypsin-like-site, their hydrolysis is less dependent on gate opening than the basic and acidic substrates, whose entry is rate-limiting. Although we were unable to determine the half-maximal binding constant or a proper V_{max} for the trypsin-like activity because saturation could not be reached, we did not observe a change in binding affinity for the caspase or the chymotrypsin substrate, yet observed changes in V_{max} for the caspase substrate, arguing for a model in which Blm10-mediated stimulation of peptide hydrolysis does not originate from an allosteric effect on the active sites. These results are consistent with an active gate-opening mechanism induced by Blm10 and are corroborated by the observation that ct-Blm10 could not activate peptide hydrolysis in open-gated CP mutants (Fig. 1*B*).

Mitochondria-related Phenotypes of Blm10 C-terminal Mutants and of Blm10 Overexpression—We reported recently that a chimeric Blm10 protein, where the last seven residues were exchanged against the corresponding residues in PA26 (Blm10PA26C), allowed complex formation with the CP, yet cells expressing this protein are characterized by a loss of function phenotype (24). Purification resulted in low yields of intact Blm10PA26C-CP complexes, which might be indicative of reduced binding affinity (24). To improve the purification yield, we substituted the endogenous promoter of the mutant with the overexpressing promoter of *GAL1*; however, the yield of intact complexes remained low (supplemental Fig. S1). Because a biochemical characterization was therefore impeded, we studied potential effects of this mutation *in vivo* by comparing growth-related phenotypes of cells overexpressing *BLM10* or the *BLM10PA26C* chimera.

To investigate potential epistatic effects with proteasome hypomorphs, we generated the same strains deleted for the proteasome-related transcription factor Rpn4. *rpn4*Δ cells are characterized by a reduced proteasome pool (34, 35). If the overexpression of *BLM10* or *BLM10PA26C* causes proteasome dysfunction, the phenotype should be exacerbated in cells deleted for *RPN4*.

Blm10 has recently been implicated in mitochondrial function and oxidative metabolism because loss of *BLM10* results in a high frequency of cells with dysfunctional mitochondria (20). We observed decreased viability of cells overexpressing *BLM10* during growth on nonfermentable carbon sources at higher temperature in the absence of *RPN4* (Fig. 4*A*, *lower panel*). The data support a role for Blm10 in correct maintenance of mitochondrial activity and indicate that this function is linked to the proteasome. Loss of *BLM10*, on the other hand, did not result in significant growth defects under these conditions.

The C terminus of PA26 is unable to induce gate opening. Thus, replacing the last seven residues of Blm10 with the corresponding residues in PA26 should abrogate the gate-opening function of Blm10. Consistent with this hypothesis. we observed a gain-of-function phenotype in cells overexpressing the Blm10PA26 chimera. After induction of the gene in the

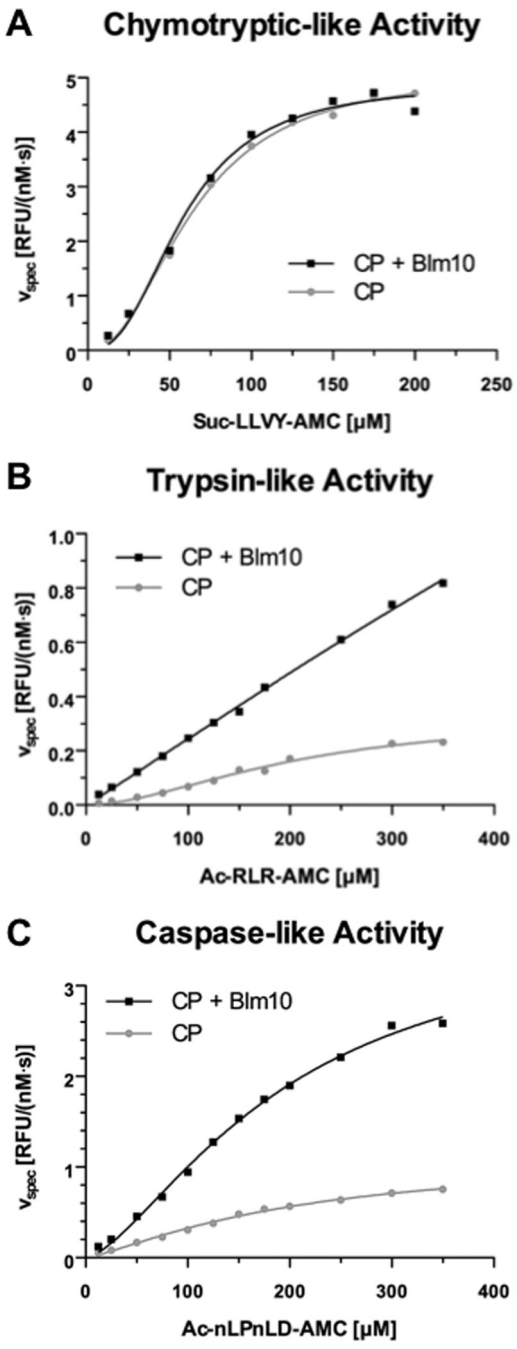

	CP	CP + Blm10
V_{max}	5.09	4.89
K_{half}	64.1	58.5
R^2	0.9983	0.9920

	CP	CP + Blm10
V_{max}	0.33	~ 7.20
K_{half}	208.6	~ 2437.0
R^2	0.9895	0.9982

	CP	CP + Blm10
V_{max}	1.14	3.75
K_{half}	204.8	194.5
R^2	0.9956	0.9967

FIGURE 3. **Impact of Blm10 on the different proteasomal peptidase activities.** Substrate kinetics were determined using purified CP and Blm10-CP with varying concentrations of Suc-LLVY-AMC to determine the chymotrypsin-like activity (*A*), Ac-RLR-AMC for trypsin-like activity (*B*), and Ac-nLPnLD-AMC for caspase-like activity (*C*). The kinetic parameters of each reaction are shown in the tables to the *right*.

presence of galactose, the cells were not viable at higher temperature or on nonfermentable carbon sources (YPGly). Furthermore, co-deletion of *RPN4* aggravated the phenotype, resulting in lethality under inducing conditions (YPGal) already at normal growth temperatures (Fig. 4*A*, *upper panel*). In summary, although cells tolerate Blm10 overexpression unless oxidative metabolism is induced at higher growth temperature, elevated expression of a gating incompetent Blm10 version is toxic at higher temperature or in cells with reduced proteasome capacity as in cells deleted for *RPN4*.

Although previous reports suggested that plasmid-derived overexpression of WT Blm10 might be lethal (33) or might result in a slow growth phenotype (21), overexpression from the genomic locus (*GAL1pBLM10*) did not produce a visible phenotype at normal growth temperature under the conditions chosen (Fig. 4*A*, *upper panel*). Because the lethal phenotype was previously speculated to be caused by blocking RP-binding sites in the presence of elevated Blm10 levels (33), we investigated proteasomal complex formation in cells overexpressing *BLM10* via native gel electrophoresis in unfractionated lysates. Although we observed a partial reduction in RP_2-CP complexes, the dominant change upon Blm10 overexpression was a complete shift of the RP-CP band to the hybrid Blm10-CP-RP complex (Fig. 4*B*). This finding argues for a model in which

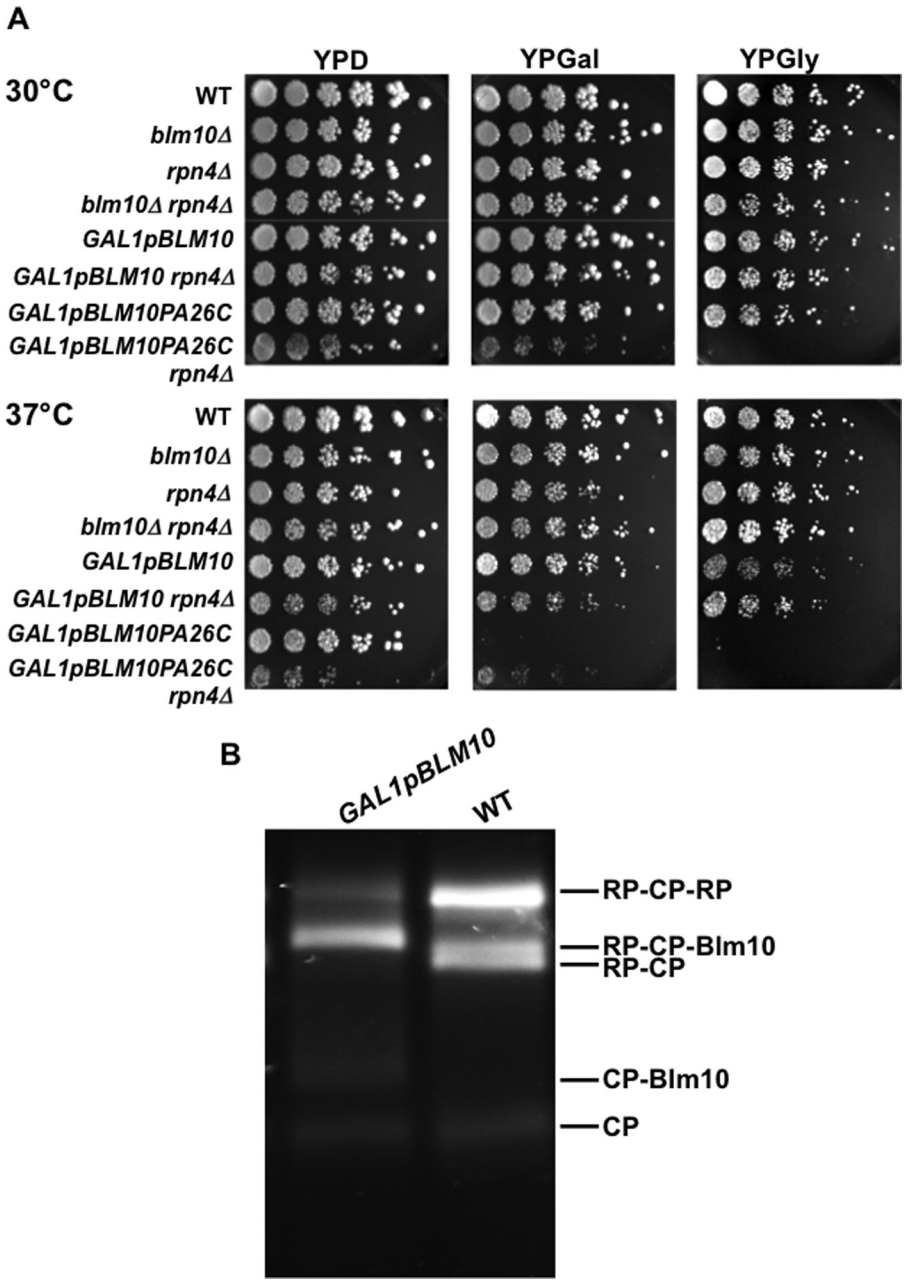

FIGURE 4. **Phenotypic characterization of cells overexpressing Blm10 or a gating incompetent Blm10PA26 chimera.** *A*, the strains indicated were grown in YPD and spotted on complete media with glucose (YPD) as control, galactose (YPGal) to induce Blm10 overexpression, and glycerol as carbon source for analysis of nonfermentative growth. The plates were incubated either at 30 °C (*upper panel*) or at 37 °C (*lower panel*). *B*, the strains indicated were subjected to the same analysis as described for Fig. 2*B* to visualize the different proteasome holocomplexes.

Blm10 preferentially interacts with the unoccupied surface of RP-CP complexes rather than competing for RP binding. A significant population of Blm10-CP species without co-associated RP was not observed (Fig. 4*B*).

Doubly Capped Blm10-CP Complexes Retain Proteasomal Peptidase Activity—Recently, a study performed on Blm10-CP in unfractionated lysates or with reconstituted complexes suggested that although the binding of one Blm10 promotes the peptidase activity of the CP, Blm10 binding to both ends of the cylinder inhibits CP activity (36). This model is difficult to reconcile with a proposed function of Blm10 as a proteasome activator and is not supported by an x-ray crystallographic study, which demonstrates that both gates are partially open in CP flanked on both ends with Blm10 (20). To assess this model, we purified endogenous Blm10-CP complexes under conditions that yielded a high portion of doubly capped Blm10-CP (Fig. 5*A*). The contribution of the different complexes toward CP peptidase stimulation was evaluated through an *in situ* analysis, where we determined the peptidase activity and the relative protein content after an in-gel activity assay (Fig. 5*A*, *top two panels*). Because of its broad linear dynamic range, protein content was assessed with the fluorogenic dye SYPRO Ruby. To ascertain that all of the signals analyzed were in the linear range, we performed standard curves for fluorescence increase after cleavage of the fluorogenic peptide Suc-LLVY-AMC by the CP, as well as for protein stain using Sypro Ruby (supplemental Fig. S2). As

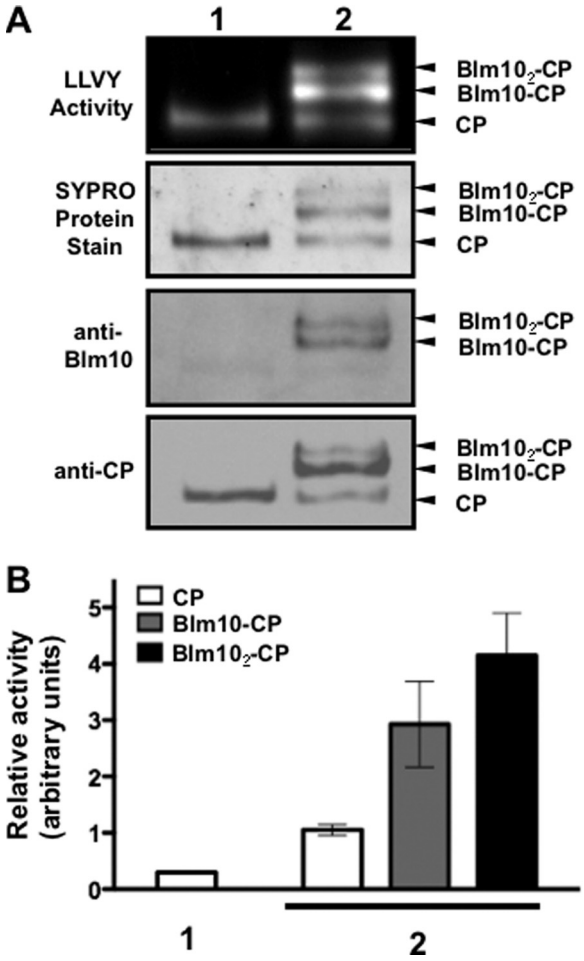

FIGURE 5. **Proteasome peptidase activity in singly and doubly capped Blm10-CP.** *A*, equal molar quantities of CP or Blm10 CP were separated by native gel electrophoresis. Peptidase activity was visualized by an in-gel activity assay (*top panel*), and protein concentration was assessed with Sypro Ruby (*second panel*). The picture of the Sypro Ruby stain is presented in a black and white inverted version. Parallel gels were subjected to immunoblotting using anti-Blm10 (*third panel*) or anti-CP antibodies. *B*, signals obtained from *A* were quantified using ImageJ. The means of three independent experiments are presented. The different values obtained for free CP present in *lanes 1* and *2* represent differences in the latency of the CP.

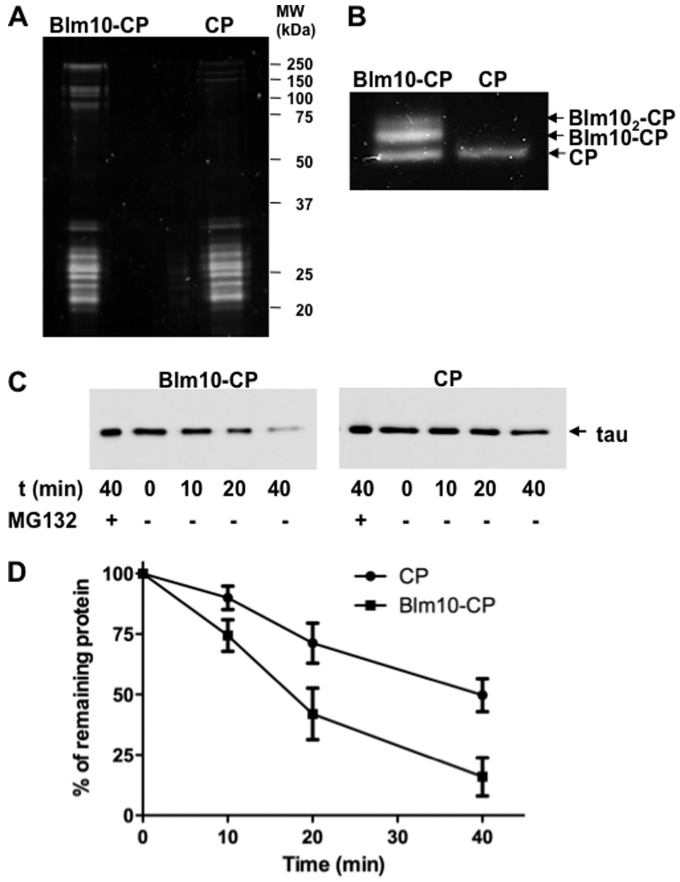

FIGURE 6. **Accelerated *in vitro* degradation of tau-441 by Blm10 proteasomes.** *A*, equal molar amounts of Blm10-CP or CP were separated by SDS-PAGE and stained with Sypro Ruby to demonstrate that equal amounts of CP were present in the assay. *B*, proteasomal complex composition was assessed by native gel electrophoresis followed by an in-gel activity assay. *C*, tau-441 was incubated with equal molar amounts of CP or Blm10-CP in the absence or presence of MG132. Aliquots were taken at the times indicated, separated by SDS-PAGE. Tau-441 was detected by immunoblotting with a tau-specific antibody. *D*, the mean values of the densitometric analysis of three independent degradation assays are presented.

shown in Fig. 5*B*, doubly capped Blm10 proteasomes are fully active. To demonstrate that the slowest migrating complex indeed contains doubly capped Blm10-CP, we analyzed the Blm10 content in the bands with an anti-Blm10 antibody (Fig. 5*A*, *second to last panel*).

Blm10 Promotes Protein Degradation in Vitro—Cryo-EM (21) and x-ray crystallographic studies (20) revealed a fully or partially open gate upon Blm10 binding, respectively. Furthermore, the x-ray structure revealed a pore of 13 × 22 Å within the Blm10 dome. The largest opening in the PAN complex from *Methanocaldococcus jannaschii* has a diameter of 13 Å (37), and this ATPase complex promotes the degradation of unfolded proteins by the proteasome (38). Thus, we speculated that the overall topology of the Blm10-CP complex might accommodate the passage and subsequent degradation of an unstructured protein. To test this, we established an *in vitro* assay to investigate whether Blm10-CP complexes are able to promote the degradation of recombinant unstructured tau-441 (supplemental Fig. S3), a substrate that has been demonstrated to be degraded by the proteasome *in vitro* in the absence of ATP or ubiquitination (39). For this assay, equal molar amounts of CP or Blm10-CP (Fig. 6, *A* and *B*) were incubated with tau in the presence or absence of the proteasome inhibitor MG132. While in the presence of the proteasome inhibitor MG132, tau turnover was blocked, both CP and Blm10-CP complexes promoted tau degradation. Blm10-CP complexes exhibited an ~2-fold accelerated turnover of the unstructured protein (Fig. 6, *C* and *D*) as compared with CP alone. We conclude that Blm10 binding activates the proteolytic activity of the CP, resulting in a more efficient turnover of unstructured proteins.

DISCUSSION

The cylindrical proteasome core particle is assembled in a latent form and has its active sites sequestered within the interior of the cylinder (6). Stimulation of the proteolytic capacity of the CP requires its association with a proteasome activator (9). These proteins mediate structural changes in the α-ring, opening the gate to allow substrate entry. The open and the closed conformations are distinguished by the positions of the N ter-

mini of the CP α-subunits. While they form an interlaced layer in the closed form, thus occluding substrate entry, upon binding of PA26, they rotate away from the body of the cylinder and adopt an ordered 7-fold symmetric conformation in the open form (40). The structural motifs in the N-terminal portion of the α-subunits, which are involved in the gating mechanism, are the rigid helix H0, a reverse turn, and the extreme N termini of each α-subunit. Two mechanistically and structurally different strategies for proteasome gating have been reported or suggested so far. Biochemical, cryo-EM, and x-ray diffraction studies indicate that the proteasomal ATPases induce gate opening through the docking of their C termini, but their final position in the CP binding pockets has not been resolved yet (25, 26, 29–31). The crystal structure of PA26, a homolog of the mammalian PA28 proteasome activator family (11), in a complex with yeast CP revealed a different proteasome activation mechanism: although the heptameric PA26 ring still associates with the CP α-ring through their extreme C termini, activation is achieved via an internal structure, the activation loop (40, 41). It interacts with a conserved Pro-13 within the reverse turn in the proteasome α-subunits. Displacement of Pro-13 appears to drive the formation of the open pore by dislocating the reverse turn by ~1 Å, a movement that is propagated to the N termini (40).

Blm10 orthologs contain a universally conserved motif at their C termini, YY*X* or YF*X*, that is analogous to the HbY*X* motif found in proteasomal ATPases involved in CP gating. The data presented in this study demonstrate that this motif is actively involved in the CP gate-opening mechanism by Blm10 proteins. Mutagenesis in that region affects the function of Blm10. Two different phenotype classes were observed. Manipulating the penultimate tyrosine (Tyr-2142) either through deletion of the last two residues (24) or through exchange against a valine as shown in Fig. 2 abrogates proteasome binding and produces a loss of function phenotype. The same observations were made for an exchange of Ser-2140 against histidine. Exchange of Arg-2139 against an aspartate, on the other hand, promotes binding. The cells, however, exhibit a partial loss of function phenotype, which we speculate to be caused by inefficient CP gating. Similar characteristics were observed for a Blm10 chimera, where the C terminus of Blm10 was exchanged against the seven last residues of the gating-incompetent PA26 C terminus (24).

We furthermore report that a heptameric peptide derived from the Blm10 C terminus is sufficient to stimulate the peptidase activity of WT CP but not of a CP mutant with a constitutively open gate. A Blm10 C-terminal peptide where the penultimate tyrosine has been replaced by an alanine loses the ability to stimulate. These data are in agreement with a model in which docking of the C terminus of Blm10 occurs in a similar fashion as the proteasomal ATPases C termini and induces structural changes in the α-ring surface that result in gate opening. Thus, our data demonstrate that the HbY*X* motif is crucial for the Blm10 proteasome interaction as to mediate gate opening. It furthermore supports information obtained from a recent crystal structure demonstrating that the HbY*X* motif in Blm10 repositions crucial residues of the reverse turn within its binding pocket and induces a similar conformation as observed in the open conformation of the PA26-CP complex (9, 20).

Blm10 is an unusual proteasome activator because it is a monomeric protein of 246 kDa in contrast to PA28 activators or the proteasomal ATPases, which form oligomeric rings (42–44). Blm10 binding to the proteasome breaks the 7-fold pseudosymmetry of the core cylinder, because it engages only with a single binding pocket. However, breaking the CP symmetry during activation is not without precedent. Biochemical analyses of the activation capacity of the RP ATPase C termini revealed that only three of the six ATPases effectively stimulate CP activity (29), and it is likely that only one HbY*X* C terminus may interact with the CP at any given time (45). This hypothesis is supported by the finding that although the C terminus of Rpt3 does contain a HbY*X* motif, its function appears to be restricted to CP docking rather than gating (46). These reports argue for a mechanism in which an asymmetric engagement of the activator binding pockets within the α-ring surface is sufficient for gate opening, although in the case of the RP, the binding of ubiquitin conjugates somehow further enhances gate opening and substrate entry (47).

In summary, whereas all proteasome activators bind via their C termini to the same binding pockets located at the CP surface, two different gate opening mechanisms can be used: C-terminal docking-mediated activation by the proteasomal ATPases and Blm10 and activation loop-mediated gate opening by the PA26/PA28 family of proteasome activators. Mechanistically, proteasome activators can also be classified according to whether they possess ATPase activity or not. Even an open CP gate allows only restricted access to the internal degradation chamber of the proteasome, and substrate proteins must be unfolded before they can enter (38, 43, 48). The proteasomal ATPases within the RP and PAN are able to perform this activity, whereas PA28 and Blm10 activators do not.

Very few targets for PA28 have been described (49), and there is little information on which substrates are specifically degraded by Blm10 proteasomes. The only protein so far that has been reported to require Blm10 for correct proteasome-mediated turnover is the ribosome-related transcription factor Sfp1 (24). Many transcription factors or transcriptional co-regulators are predicted to contain large intrinsically unstructured regions (50). The graphic webserver FoldIndex© (51) provides an algorithm to predict unstructured regions in proteins based on their primary sequence. Such an analysis of the Sfp1 sequence predicts a high portion of intrinsically unstructured regions (supplemental Fig. S3*A*). A preference for degrading unstructured proteins might explain the lack of ATPase activity in Blm10 activators. This hypothesis is corroborated by our findings that Blm10 is able to stimulate CP-mediated degradation of the unstructured proteasome substrate tau-441 (supplemental Fig. S3*B*) *in vitro* as shown in this report. We infer from these data that the structural change of the CP gate upon Blm10 binding is sufficient for passage of both peptides and unfolded protein substrates. We propose that the ability of Blm10 proteasomes to promote the degradation of unfolded proteasome substrates might represent a critical and perhaps principal function of Blm10 *in vivo*.

Acknowledgment—We thank Attila Vereb for technical support.

REFERENCES

1. Finley, D. (2009) *Annu. Rev. Biochem.* **78,** 477–513
2. Pickart, C. M., and Cohen, R. E. (2004) *Nat. Rev. Mol. Cell Biol.* **5,** 177–187
3. Wolf, D. H., and Hilt, W. (2004) *Biochim. Biophys. Acta* **1695,** 19–31
4. Schwartz, A. L., and Ciechanover, A. (2009) *Annu. Rev. Pharmacol. Toxicol.* **49,** 73–96
5. Schmidt, M., Hanna, J., Elsasser, S., and Finley, D. (2005) *Biol. Chem.* **386,** 725–737
6. Groll, M., Ditzel, L., Löwe, J., Stock, D., Bochtler, M., Bartunik, H. D., and Huber, R. (1997) *Nature* **386,** 463–471
7. Kisselev, A. F., Callard, A., and Goldberg, A. L. (2006) *J. Biol. Chem.* **281,** 8582–8590
8. Groll, M., Bajorek, M., Köhler, A., Moroder, L., Rubin, D. M., Huber, R., Glickman, M. H., and Finley, D. (2000) *Nat. Struct. Biol.* **7,** 1062–1067
9. Stadtmueller, B. M., and Hill, C. P. (2011) *Mol. Cell* **41,** 8–19
10. Rechsteiner, M., and Hill, C. P. (2005) *Trends Cell Biol.* **15,** 27–33
11. Yao, Y., Huang, L., Krutchinsky, A., Wong, M. L., Standing, K. G., Burlingame, A. L., and Wang, C. C. (1999) *J. Biol. Chem.* **274,** 33921–33930
12. Ustrell, V., Hoffman, L., Pratt, G., and Rechsteiner, M. (2002) *EMBO J.* **21,** 3516–3525
13. Schmidt, M., Haas, W., Crosas, B., Santamaria, P. G., Gygi, S. P., Walz, T., and Finley, D. (2005) *Nat. Struct. Mol. Biol.* **12,** 294–303
14. Blickwedehl, J., Agarwal, M., Seong, C., Pandita, R. K., Melendy, T., Sung, P., Pandita, T. K., and Bangia, N. (2008) *Proc. Natl. Acad. Sci. U.S.A.* **105,** 16165–16170
15. Hendil, K. B., Khan, S., and Tanaka, K. (1998) *Biochem. J.* **332,** 749–754
16. Kopp, F., Dahlmann, B., and Kuehn, L. (2001) *J. Mol. Biol.* **313,** 465–471
17. Hartmann-Petersen, R., Tanaka, K., and Hendil, K. B. (2001) *Arch. Biochem. Biophys.* **386,** 89–94
18. Cascio, P., Call, M., Petre, B. M., Walz, T., and Goldberg, A. L. (2002) *EMBO J.* **21,** 2636–2645
19. Kajava, A. V., Gorbea, C., Ortega, J., Rechsteiner, M., and Steven, A. C. (2004) *J. Struct. Biol.* **146,** 425–430
20. Sadre-Bazzaz, K., Whitby, F. G., Robinson, H., Formosa, T., and Hill, C. P. (2010) *Mol. Cell* **37,** 728–735
21. Iwanczyk, J., Sadre-Bazzaz, K., Ferrell, K., Kondrashkina, E., Formosa, T., Hill, C. P., and Ortega, J. (2006) *J. Mol. Biol.* **363,** 648–659
22. Ortega, J., Heymann, J. B., Kajava, A. V., Ustrell, V., Rechsteiner, M., and Steven, A. C. (2005) *J. Mol. Biol.* **346,** 1221–1227
23. Marques, A. J., Glanemann, C., Ramos, P. C., and Dohmen, R. J. (2007) *J. Biol. Chem.* **282,** 34869–34876
24. Lopez, A. D., Tar, K., Krügel, U., Dange, T., Ros, I. G., and Schmidt, M. (2011) *Mol. Biol. Cell* **22,** 528–540
25. Rabl, J., Smith, D. M., Yu, Y., Chang, S. C., Goldberg, A. L., and Cheng, Y. (2008) *Mol. Cell* **30,** 360–368
26. Yu, Y., Smith, D. M., Kim, H. M., Rodriguez, V., Goldberg, A. L., and Cheng, Y. (2010) *EMBO J.* **29,** 692–702
27. Longtine, M. S., McKenzie, A., 3rd, Demarini, D. J., Shah, N. G., Wach, A., Brachat, A., Philippsen, P., and Pringle, J. R. (1998) *Yeast* **14,** 953–961
28. Goldstein, A. L., and McCusker, J. H. (1999) *Yeast* **15** 1541–1553
29. Smith, D. M., Chang, S. C., Park, S., Finley, D., Cheng, Y., and Goldberg, A. L. (2007) *Mol. Cell* **27,** 731–744
30. Gillette, T. G., Kumar, B., Thompson, D., Slaughter, C. A., and DeMartino, G. N. (2008) *J. Biol. Chem.* **283,** 31813–31822
31. Park, S., Roelofs, J., Kim, W., Robert, J., Schmidt, M., Gygi, S. P., and Finley, D. (2009) *Nature* **459,** 866–870
32. Kisselev, A. F., Kaganovich, D., and Goldberg, A. L. (2002) *J. Biol. Chem.* **277,** 22260–22270
33. Fehlker, M., Wendler, P., Lehmann, A., and Enenkel C (2003) *EMBO Rep.* **4,** 959–963
34. Dohmen, R. J., Willers, I., Marques, A. J. (2007) *Biochim. Biophys. Acta* **1773,** 1599–1604
35. Kruegel, U., Robison, B., Dange, T., Kahlert, G., Delaney, J. R., Kotireddy, S., Tsuchiya, M., Tsuchiyama, S., Murakami, C. J., Schleit, J., Sutphin, G., Carr, D., Tar, K., Dittmar, G., Kaeberlein, M, Kennedy B. K., and Schmidt, M. (2011) *PLoS Genet.* **7,** e1002253
36. Lehmann, A., Jechow, K., and Enenkel, C. (2008) *EMBO Rep.* **9,** 1237–1243
37. Zhang, F., Hu, M., Tian, G., Zhang, P., Finley, D., Jeffrey, P. D., and Shi, Y. (2009) *Mol. Cell* **34,** 473–484
38. Smith, D. M., Kafri, G., Cheng, Y., Ng, D., Walz, T., and Goldberg, A. L. (2005) *Mol. Cell* **20,** 687–698
39. David, D. C., Layfield, R., Serpell, L., Narain, Y., Goedert, M., and Spillantini, M. G. (2002) *J. Neurochem.* **83,** 176–185
40. Förster, A., Masters, E. I., Whitby, F. G., Robinson, H., and Hill, C. P. (2005) *Mol. Cell* **18,** 589–599
41. Whitby, F. G., Masters, E. I., Kramer, L., Knowlton, J. R., Yao, Y., Wang, C. C., and Hill, C. P. (2000) *Nature* **408,** 115–120
42. Knowlton, J. R., Johnston, S. C., Whitby, F. G., Realini, C., Zhang, Z., Rechsteiner, M., and Hill, C. P. (1997) *Nature* **390,** 639–643
43. Liu, C. W., Millen, L., Roman, T. B., Xiong, H., Gilbert, H. F., Noiva, R., DeMartino, G. N., and Thomas, P. J. (2002) *J. Biol. Chem.* **277,** 26815–26820
44. Tomko, R. J., Jr., Funakoshi, M., Schneider, K., Wang, J., and Hochstrasser, M. (2010) *Mol. Cell* **38,** 393–403
45. Smith, D. M., Fraga, H., Reis, C., Kafri, G., and Goldberg, A. L. (2011) *Cell* **144,** 526–538
46. Kumar, B., Kim, Y. C., and DeMartino, G. N. (2010) *J. Biol. Chem.* **285,** 39523–39535
47. Peth, A., Besche, H. C., and Goldberg, A. L. (2009) *Mol. Cell* **36,** 794–804
48. Braun, B. C., Glickman, M., Kraft, R., Dahlmann, B., Kloetzel, P. M., Finley, D., Schmidt, M. (1999) *Nat. Cell Biol.* **1,** 221–226
49. Li, X., Amazit, L., Long, W., Lonard, D. M., Monaco, J. J., and O'Malley, B. W. (2007) *Mol. Cell* **26,** 831–842
50. Dyson, H. J., and Wright, P. E. (2005) *Nat. Rev. Mol. Cell Biol.* **6,** 197–208
51. Prilusky, J., Felder, C. E., Zeev-Ben-Mordehai, T., Rydberg, E. H., Man, O., Beckmann, J. S., Silman, I., and Sussman, J. L. (2005) *Bioinformatics* **21,** 3435–3438
52. Brachmann, C. B., Davies, A., Cost, G. J., Caputo, E., Li, J., Hieter, P., and Boeke, J. D. (1998) *Yeast* **14,** 115–132

Blm10 Protein Promotes Proteasomal Substrate Turnover by an Active Gating Mechanism

Thomas Dange, David Smith, Tahel Noy, Philipp C. Rommel, Lukas Jurzitza, Radames J. B. Cordero, Anne Legendre, Daniel Finley, Alfred L. Goldberg and Marion Schmidt

J. Biol. Chem. 2011, 286:42830-42839.
doi: 10.1074/jbc.M111.300178 originally published online October 24, 2011
